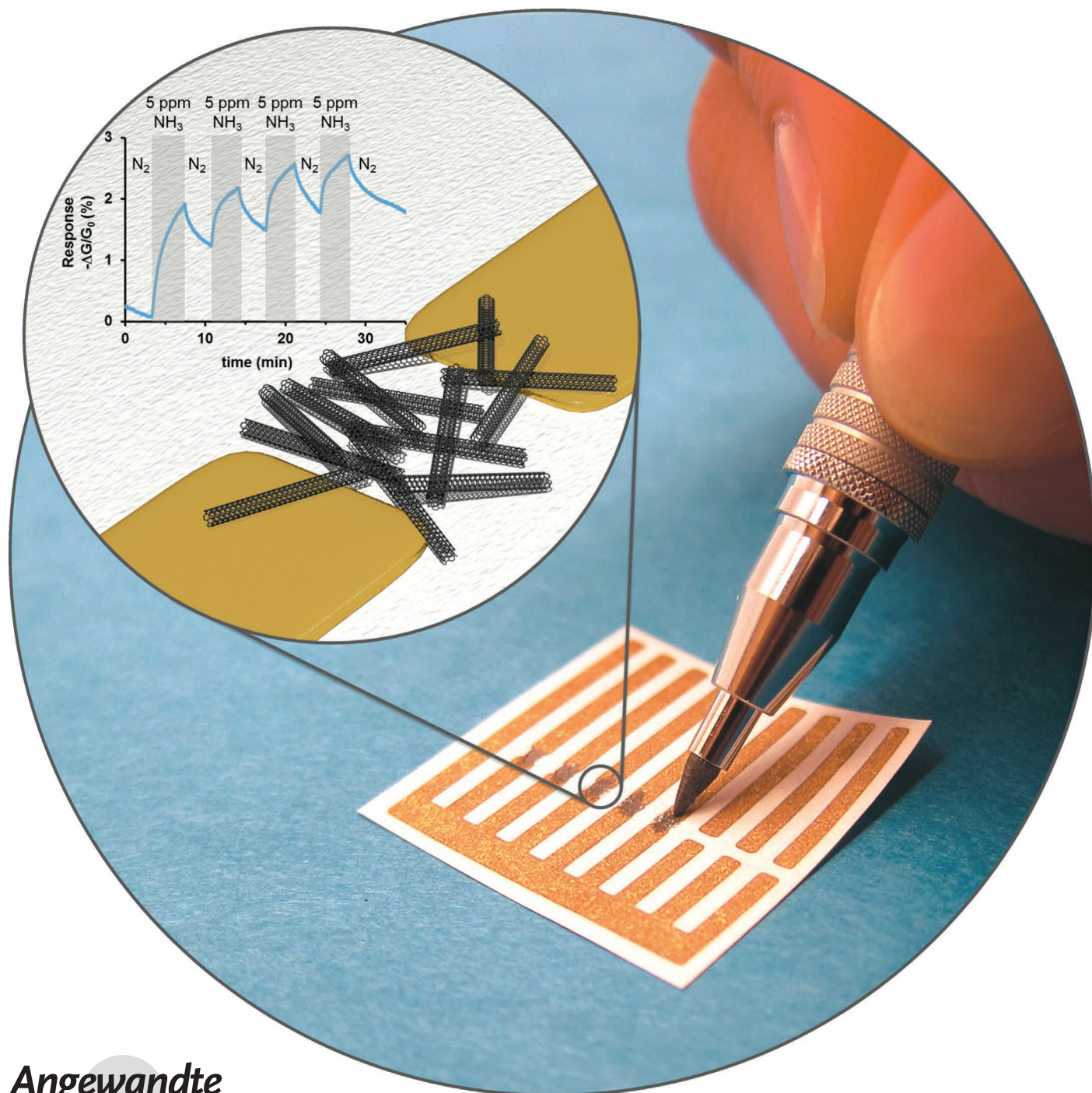


Mechanical Drawing of Gas Sensors on Paper**

Katherine A. Mirica, Jonathan G. Weis, Jan M. Schnorr, Birgit Esser, and Timothy M. Swager*



The detection and identification of gases and volatile organic compounds (VOCs) are critically important to human health and safety.^[1–4] Gas chromatography mass spectrometry (GC–MS) is a reliable and established technology for analyzing gases and VOCs.^[1] This method is highly sensitive and capable of resolving and identifying complex mixtures of analytes. The GC–MS method suffers from several limitations. The instruments are expensive and bulky, and highly trained technicians are required to carry out detection and analysis. Alternative sensors for detecting gases and VOCs rely on changes in either electrical, gravimetric, or optical signals.^[2,3] These existing systems, however, involve tradeoffs in terms of cost, portability, reproducibility, requirements for calibration, sensitivity to humidity and temperature, limited shelf life, costs for training and maintenance, and ease of use by the operator.^[3]

Nanostructured forms of carbon, such as carbon nanotubes (CNTs), are an emerging class of materials with utility in chemical sensing.^[4,5] A useful feature of these materials is that their electrical conductance is extremely sensitive to changes in the local chemical environment.^[6–8] Resistivity-based CNT sensors offer significant advantages over other methods for detecting gases and VOCs in terms of portability, ease of use, cost, and suitability for room-temperature operation.^[4,5] A number of drawbacks, however, such as the dependence on expensive specialized equipment for the fabrication of devices, the need for solution processing, the low solubility of CNTs in most solvents, and the limited stability of CNT-based dispersions, restrict applications of these materials. Overcoming these drawbacks by developing a method for fabricating sensors from carbon-based materials that has the characteristics of being operationally simple, inexpensive, versatile, and solvent-free should have a significant impact on widening the range of applications and commercial opportunities of these materials.

Our approach for overcoming the challenges of working with CNTs relies on a simple solvent-free method operationally analogous to drawing with a pencil on paper. The method involves the fabrication of chemiresistive gas sensors by mechanical abrasion of compressed powders of sensing materials on the fibers of cellulose. We illustrate this approach by depositing conductive layers of several forms of carbon (e.g., single-walled carbon nanotubes (SWCNTs), multiwalled carbon nanotubes, and graphite) on the surface of

different papers (Figure 1, Figure S1 in the Supporting Information).

We chose paper as the substrate for the fabrication of our sensors because 1) it is one of the most ubiquitous and least expensive materials;^[9] 2) it is compatible with several forms of printing and surface-processing technologies;^[9–11] 3) it has a proven utility as a substrate for sensors and electronic devices;^[6,9,10,12,13] and 4) it is a common substrate for abrasion-based writing and drawing with graphite and wax-based pencils.^[14] We chose to focus this study on generating sensors from pristine SWCNTs as they: 1) are extremely sensitive to differences in the chemical composition of their surrounding environment,^[6–8] 2) are commercially available, 3) and can be chemically modified in a covalent^[15] and noncovalent^[16] fashion to generate selective sensors.^[17] We chose to evaluate the performance of our devices with gaseous NH₃, because it is an important industrial hazard and interacts strongly with pristine SWCNTs through charge transfer that decreases the conductance of CNTs.^[4]

Several studies have also focused on fabricating CNT-based sensors on the surface of paper.^[6,13,18] The existing approaches, however, typically rely on solution-based deposition (e.g., drop-casting, dip-coating, ink-jet printing) of CNTs on paper, and suffer from one or more disadvantages that include the limited chemical stability of the “ink”, the use of hazardous chemical solvents, surfactants, or polymeric additives for dispersing CNTs in solution, and the requirement for ultrasonication, which can cause structural damage to CNTs. Although a solvent-free deposition of CNTs by mechanical abrasion on the surface of paper has remained unexplored until this report, several examples from the literature demonstrate related concepts using other types of materials and substrates. For instance, Albrecht and Lyding demonstrated the solvent-free transfer of SWCNTs from a fiberglass sheath impregnated with nanotube powder to the surface of a hydrogen-passivated Si(100),^[19] and Alvarez et al. demonstrated that abrasion of Fe metal on the surface of Al₂O₃/SiO₂ can be used to pattern the Fe catalyst for facilitating the synthesis of CNTs by chemical vapor deposition.^[20] We believe that these reports, along with the work we present here, suggest that the general strategy of fabricating functional devices by mechanical abrasion can be extended to many types of materials and substrates.

Figure 1 shows sensors fabricated by manual mechanical abrasion of a pellet of compressed SWCNTs on the surfaces of four types of paper. To create the pellet, we compressed 100 mg of commercially obtained SWCNTs in a die by applying a constant pressure of 0.4 GPa with a hydraulic press for one minute. To fabricate the sensors, we first deposited gold electrodes (with a 1 mm gap between the electrodes) on the surface of paper by thermal evaporation through a shadow mask. We then distributed SWCNTs on the surface of paper within the gap between the gold electrodes by abrading the pellet (at a rate of roughly 10 mm s⁻¹ with an applied force of 1–5 N) several times to obtain the desired resistance of devices (typically 10–30 kΩ for the devices used in this study). Precise control over the rate of deposition or the applied force was not necessary, and the data we present herein is for devices we prepared by hand. We obtained good

[*] Dr. K. A. Mirica, J. G. Weis, Dr. J. M. Schnorr, Dr. B. Esser, Prof. Dr. T. M. Swager
 Department of Chemistry
 and Institute for Soldier Nanotechnologies
 Massachusetts Institute of Technology
 Cambridge, MA 02139 (USA)
 E-mail: tswager@mit.edu

[**] This work was supported by the Army Research Office through the Institute for Soldier Nanotechnologies (W911NF-07-D-004), the National Institute of Health and the National Cancer Institute (postdoctoral fellowship to K.A.M.; grant number F32A1571997), and the German Academy of Sciences (postdoctoral fellowship to B.E.; LPDS 2009-8).



Supporting information for this article is available on the WWW under <http://dx.doi.org/10.1002/anie.201206069>.

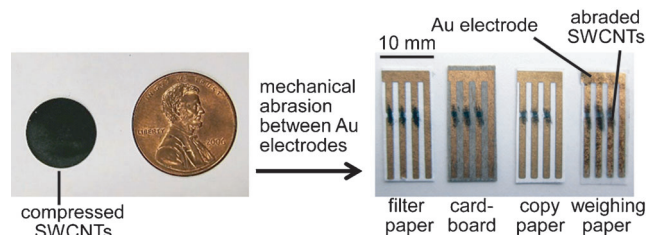


Figure 1. Fabrication of sensors on various types of paper by the mechanical abrasion of a pellet of compressed SWCNTs.

reproducibility (5%) in sensing response between devices that ranged in resistance between 10 and 30 k Ω .

We examined seven types of cellulose-based paper that differed in surface roughness and purity to define the optimal characteristics of the substrate for these types of sensors. The papers chosen for this study had different values of root-mean-square surface roughness ($R_{\text{rms}} \approx 2\text{--}10 \mu\text{m}$), as measured by profilometry, and varied in the extent of purity of the cellulose (see Table S1 and Figure S4 in the Supporting Information for details). We used FTIR, elemental analysis, and fluorescence under UV light to characterize the purity of the cellulose used in this study. Despite significant difference in surface roughness and appearance, filter paper ($R_{\text{rms}} = 9.6 \pm 0.2 \mu\text{m}$) and weighing paper ($R_{\text{rms}} = 2.0 \pm 0.5 \mu\text{m}$) contained highly pure cellulose (>95%) and were chemically indistinguishable by FTIR spectroscopy and elemental analysis. The remaining types of paper contained additives and dyes detectable by FTIR at 1400–1500 cm^{-1} and cellulose with purity varying between 75–90% as indicated by elemental analysis. Furthermore, several papers (e.g., two types of copy paper) exhibited strong fluorescence under UV light, which indicated the presence of UV-active optical brighteners. Taken together, these characteristics provide additional parameters beyond R_{rms} that could affect the performance of the devices in this study.

We characterized the morphology of the abraded SWCNTs on the surface of paper using various forms of microscopy (Figure 2 and Figures S2 and S3). Scanning electron microscopy (SEM) images (Figure 2A,B, panels I and II) show that SWCNTs abrade predominantly on the surface of the outermost cellulose fibers. We used two different methods to estimate the thickness of the abrasion layer (t) for different types of paper: 1) examination of cross-sections of devices with an optical microscope and 2) application of Equation (1). In this equation, V [cm^3] is the volume

$$t = (V/A) = m/(\rho A) \quad (1)$$

of the carbon-based abrasion layer on the surface of the paper, A [cm^2] is the surface area of the abrasion layer, m is the mass [g] of the SWCNTs on the surface of paper, and ρ [g cm^{-3}] is the density of the SWCNTs.

Visual inspection of cross-sections of devices with an optical microscope gave an estimate of $t \approx 1\text{--}10 \mu\text{m}$ (Figure 2A,B, panel III). Because the thickness of the abrasion layer is non-uniform throughout the cross-section of the device and could be non-uniformly perturbed during the

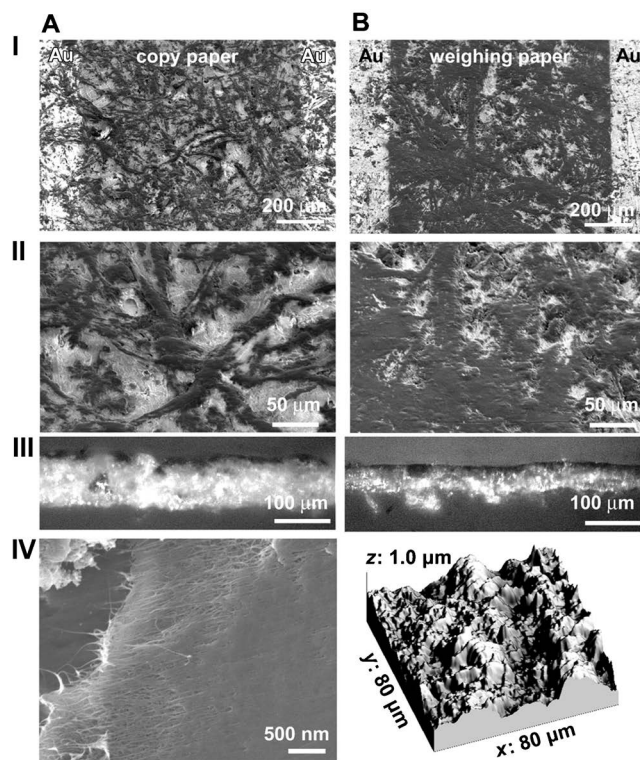


Figure 2. Imaging and characterization of sensors fabricated by the mechanical abrasion of pristine SWCNTs on copy paper (A) and weighing paper (B). I, II) SEM images of SWCNTs abraded on copy paper (A) and weighing paper (B). III) Optical micrographs of cross-sections of copy paper (A) and weighing paper (B) containing SWCNTs deposited by abrasion. IV) High-magnification SEM image of SWCNTs abraded on the surface of copy paper (A), and an AFM image of SWCNTs abraded on the surface of weighing paper (B).

process of cross-sectioning, we also obtained additional estimates of average t using Equation (1). For devices with similar resistance ($R = 14 \pm 5 \text{ k}\Omega$) fabricated by the abrasion of SWCNTs on the surface of seven different types of paper, the mass of SWCNTs per device ranged between 0.6–7 μg , and corresponding values of t were 0.1–1.9 μm (see the Supporting Information for details). Both m and t qualitatively correlate with the surface roughness of papers, such that weighing paper—the substrate with the lowest value of R_{rms} examined in this study—has lowest values of $m = 0.6 \mu\text{g}$ and $t = 0.1 \mu\text{m}$.

High-resolution SEM images confirmed the presence of densely packed bundles of SWCNTs within the abrasion layer on copy paper (Figure 2A, panel IV). We also used atomic force microscopy (AFM) to examine the surface roughness of the abrasion layer deposited on weighing paper. Panel IV in Figure 2B shows that the height of the features on the surface of the abrasion layer does not exceed 750 nm (also see Figure S3 in the Supporting Information).

After analyzing the abraded SWCNT films, we evaluated the performance of the sensors by monitoring their response towards NH_3 . We applied a small voltage (0.1 V) across the two electrodes of the devices and measured the resulting current using a potentiostat (see the Supporting Information for details). We then calculated the normalized response of

the sensors $-\Delta G/G_0$ [%] using Equation (2). In this equation,

$$-\Delta G/G_0 [\%] = [(I_0 - I)/I_0] 100 \quad (2)$$

I_0 [μA] is the initial current before exposure to the analyte and I [μA] is the current after exposure to the analyte.

Figure 3 summarizes the effect of the paper-based substrate on the signal-to-noise ratio (SNR), sensitivity, and theoretical limit of detection (LOD) of devices fabricated by mechanical abrasion of compressed SWCNTs on various types of paper. Figure 3A shows the normalized response ($-\Delta G/G_0$ [%]) of devices comprising pristine SWCNTs abraded on three different kinds of papers upon exposure to 0.5 and 5 ppm NH_3 (see Figure S7 for additional data on other types of paper for $[\text{NH}_3] = 0.5\text{--}5000$ ppm). The sensing traces for each type of paper show overlaid responses from two sensors. Simple inspection of this data reveals that the sensors exhibit good reproducibility in response towards NH_3 for each type of paper.

The response of SWCNTs towards NH_3 (Figure 3A) exhibits two notable features on all types of paper. First, the magnitude of the response (i.e., the height of the peak in the $-\Delta G/G_0$ versus time plot indicated by the gray arrows in Figure 3A) during the first exposure to NH_3 is higher than for subsequent exposures. Second, the sensors exhibit an apparent baseline drift during exposure to NH_3 (i.e., the value of $-\Delta G/G_0$ at the baseline in Figure 3A increases after each exposure to NH_3). Both of these features are intrinsic characteristics of devices based on random networks of pristine SWCNTs and are a consequence of the fact that the interaction of pristine SWCNTs with NH_3 is not fully reversible on the time scale of this type of experiment.^[21] When measuring the response of our sensors, we disregard the first exposure of the sensor to the analyte and calculate the response based on the three (or more) subsequent exposures.

All sensors examined in this study showed a linear response for $[\text{NH}_3] = 0.5\text{--}10$ ppm, and a nonlinear response for $[\text{NH}_3] > 10$ ppm (Figure 3B,C, and Figure S9). As evident from Figure 3A–C, the choice of paper has a strong effect on the signal-to-noise ratio and the sensitivity of sensors towards NH_3 across a wide range of concentrations. Weighing paper—the substrate with the lowest value of R_{rms} examined in this study—gave the highest SNR (Figure 3A) and the highest sensitivity across a range of concentrations (0.5–5000 ppm; Figure 3B,C) in response to NH_3 . Conversely, filter paper—the substrate with the highest value of R_{rms} examined in this study—gave the lowest SNR (Figure 3A) and the lowest sensitivity across a range of concentrations (Figure 3B,C) towards NH_3 . Because these two papers are chemically indistinguishable, we hypothesized that physical properties (e.g., R_{rms}) rather than chemical properties (e.g., presence of chemical impurities or optical brighteners on the surface of cellulose) play a dominant role in determining the performance of the devices in this study.

To test this hypothesis, we examined the correlation between the theoretical limit of detection towards NH_3 (see the Supporting Information for details regarding this calculation) and R_{rms} for sensors fabricated on seven different types of paper (Figure 3D). The theoretical LOD spans an order of

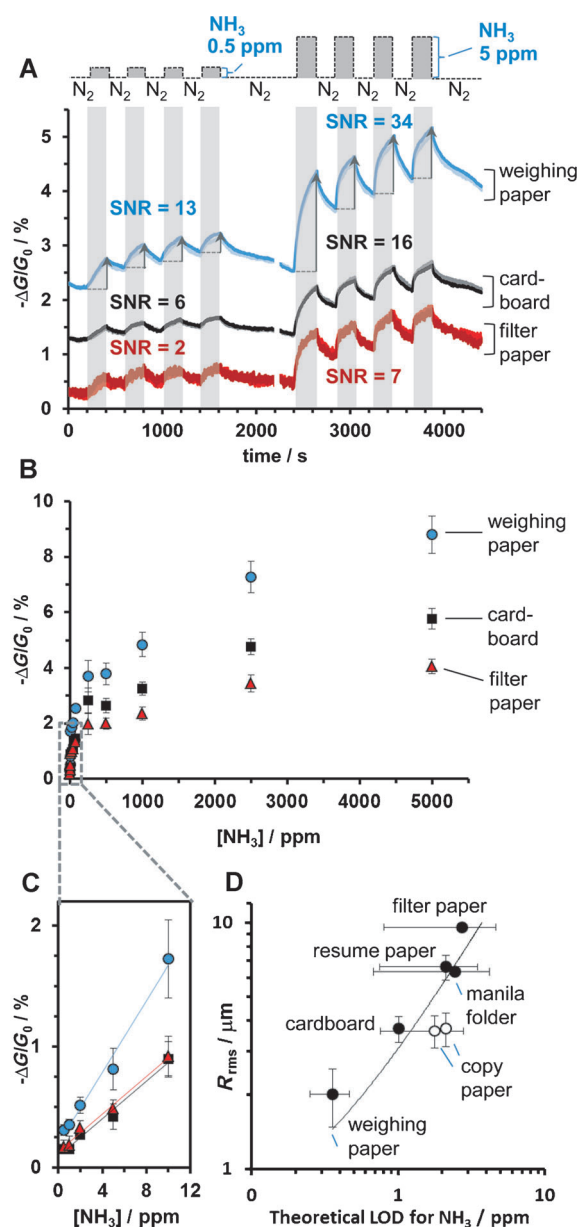


Figure 3. Response towards NH_3 gas (diluted with N_2) of sensors fabricated by mechanical abrasion of compressed pristine SWCNTs on various papers. A) Normalized change in conductance (represented as $-\Delta G/G_0$ [%]) with respect to time of devices exposed to 0.5 and 5 ppm NH_3 (4 × 200 s each). The plot shows overlays of the responses of two separate devices for each type of paper. B) Correlation of sensor response ($-\Delta G/G_0$ [%]) with $[\text{NH}_3]$ (exposed for 200 s) for devices fabricated on three different types of paper. Vertical error bars represent standard deviations from the mean based on three exposures to NH_3 of three devices on each type of paper. The contribution of the signal from the first exposure to NH_3 at each concentration is excluded from the calculations of the mean signal and the standard deviation. C) Linear range of response of sensors drawn on weighing paper, filter paper, and cardboard. $R^2 = 0.99$ for all three types of paper shown. D) Plot correlating the surface roughness of the paper substrates, on which the sensors were fabricated, with the theoretical detection limit of these sensors for NH_3 (○ = substrate is fluorescent under UV light; ● = substrate is not fluorescent).

magnitude (0.36–2.7 ppm) for seven types of paper with R_{rms} values ranging between 2–10 μm . We approximated the

correlation in Figure 3D empirically with a linear fit ($y = 2.5x + 0.5$, $R^2 = 0.68$). Weighing paper ($R_{\text{rms}} = 2.0 \pm 0.5 \mu\text{m}$) exhibits the lowest theoretical LOD of 0.36 ppm, while filter paper ($R_{\text{rms}} = 9.6 \pm 0.2 \mu\text{m}$) has an LOD of 2.7 ppm. The value of the theoretical LOD for NH_3 on weighing paper is within the same order of magnitude as the LOD values for devices based on chemically modified SWCNTs fabricated by traditional solution-phase methods on glass substrates.^[21,22]

The lowest experimentally accessible concentration of NH_3 that could be delivered reliably to our devices was 0.5 ppm. We were, therefore, unable to verify the theoretical LOD (i.e., $[\text{NH}_3]$ at which $\text{SNR} = 3$) of SWCNT-based devices drawn on weighing paper and cardboard, because these devices exhibited SNRs of as high as 13 and 6, respectively, towards 0.5 ppm NH_3 . The experimental LOD for the devices on the other types of paper examined in this study ranged between 1–3 ppm NH_3 and correlated well with the theoretical LOD.

Taken together, the results presented in Figure 3 suggest that on the basis of signal-to-noise ratio, sensitivity, and theoretical LOD towards NH_3 , weighing paper is an optimal substrate (compared to other types of papers examined in this study) for the fabrication of SWCNT-based gas sensors by mechanical abrasion. We, therefore, focused our studies of device-to-device reproducibility using SWCNT-based gas sensors drawn on weighing paper.

Figure 4 summarizes the results of these studies for a single paper-based chip containing eight devices ($R = 29 \pm 6 \text{ k}\Omega$, shown in the inset of Figure 4A). Figure 4A shows the concentration-dependent response of devices towards NH_3 at concentrations of 0.5–80 ppm. In this range of concentrations, the devices exhibit a nonlinear response towards NH_3 that begins to approach linearity for $[\text{NH}_3] < 10$ ppm.

To test the reproducibility of measurements between devices as well as the ability to make repeated measurements, we exposed the chip with eight devices to 5 ppm NH_3 seven times. Figure 4B shows the responses ($-\Delta G/G_0$ [%]) of eight devices over seven cycles of exposure towards NH_3 (each

cycle constitutes exposure to 5 ppm NH_3 for 200 s followed by recovery of devices facilitated by purging with N_2 for 200 s). The coefficient of variance between devices is $5.7 \pm 0.8\%$ for each exposure to 5 ppm NH_3 , and $5 \pm 1\%$ for $[\text{NH}_3] = 0.5\text{--}80$ ppm. As discussed above, due to only partial reversibility of the SWCNT– NH_3 interaction, the magnitude of response during the first exposure to NH_3 is higher than for subsequent exposures and evens out to a reproducible value after the first cycle (inset in Figure 4B).^[21]

In conclusion, we have developed a simple, versatile, and solvent-free approach for fabricating SWCNT-based gas sensors on the surface of cellulosic paper by mechanical abrasion. We have demonstrated that the physical properties of the paper-based substrate (e.g., surface roughness) have a significant effect on the sensitivity and the signal-to-noise ratio of the resulting devices towards NH_3 . Mechanical abrasion of SWCNTs on weighing paper—the substrate with the lowest value of surface roughness examined in this study—yielded devices with a broad dynamic range towards the detection of NH_3 (0.5–5000 ppm) and a theoretical limit of detection of 0.36 ppm. This limit of detection is within the same order of magnitude as that of devices based on chemically functionalized SWCNTs fabricated by traditional solution-phase methods on glass substrates.^[21,22] Devices drawn on weighing paper exhibit coefficients of variance between devices of $5 \pm 1\%$ (for $[\text{NH}_3] = 0.5\text{--}80$ ppm)—a value comparable to the reproducibility of SWCNT-based devices fabricated by solution-phase methods.^[6,8] The approach we describe here has a number of useful characteristics that make it a desirable method for fabricating sensors from nanostructured forms of carbon: 1) it is entirely solvent-free; 2) it is simple and inexpensive; 3) it does not require the use of specialized facilities (e.g., clean room); 4) the resulting devices are flexible, stackable, and potentially wearable; 5) the devices can be easily disposed of by incineration. We believe that this method can be adapted for the fabrication of functional devices from a wide range of materials on various surfaces.

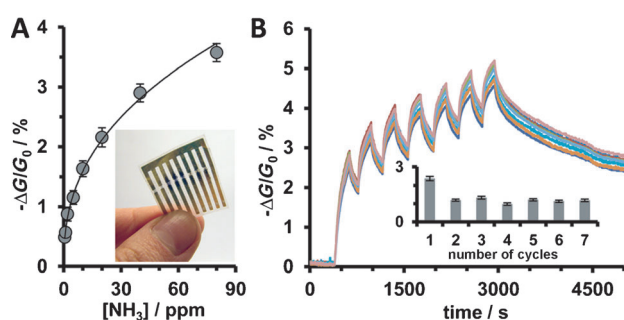


Figure 4. Response towards NH_3 gas of sensors fabricated by mechanical abrasion of compressed pristine SWCNTs on weighing paper. A) The change in conductance ($-\Delta G/G_0$ [%]) in response to NH_3 (exposed for 200 s) at low ppm concentrations. Vertical error bars represent standard deviations from the mean based on three exposures of eight devices on a single paper chip (shown in inset). B) A plot showing repeated exposure of devices shown in panel A (inset) to 5 ppm NH_3 . Vertical error bars in inset represent standard deviations from the mean response for eight devices on a single paper chip (shown in inset of panel A).

Received: July 29, 2012

Published online: October 4, 2012

Keywords: ammonia · carbon nanotubes · mechanical abrasion · paper · sensors

- [1] O. D. Sparkman, Z. E. Penton, F. G. Kitson, *Gas Chromatography and Mass Spectrometry: A Practical Guide*, Academic Press, Oxford, **2011**.
- [2] R. A. Potyrailo, C. Surman, N. Nagraj, A. Burns, *Chem. Rev.* **2011**, *111*, 7315–7354; F. Röck, N. Barsan, U. Weimar, *Chem. Rev.* **2008**, *108*, 705–725; S. E. Stitzel, M. J. Aernecke, D. R. Walt, *Annu. Rev. Biomed. Eng.* **2011**, *13*, 1–25.
- [3] A. D. Wilson, M. Baietto, *Sensors* **2009**, *9*, 5099–5148.
- [4] D. R. Kauffman, A. Star, *Angew. Chem.* **2008**, *120*, 6652–6673; *Angew. Chem. Int. Ed.* **2008**, *47*, 6550–6570.
- [5] J. M. Schnorr, T. M. Swager, *Chem. Mater.* **2011**, *23*, 646–657.
- [6] S. Ammu, V. Dua, S. R. Agnihotra, S. P. Surwade, A. Phulgirkar, S. Patel, S. K. Manohar, *J. Am. Chem. Soc.* **2012**, *134*, 4553–4556.
- [7] J. Kong, N. R. Franklin, C. Zhou, M. G. Chapline, S. Peng, K. Cho, H. Dai, *Science* **2000**, *287*, 622–625.

- [8] J. Li, Y. J. Lu, Q. Ye, M. Cinke, J. Han, M. Meyyappan, *Nano Lett.* **2003**, *3*, 929–933.
- [9] D. Tobjörk, R. Osterbacka, *Adv. Mater.* **2011**, *23*, 1935–1961.
- [10] M. C. Barr, J. A. Rowehl, R. R. Lunt, J. Xu, A. Wang, C. M. Boyce, S. G. Im, V. Bulovic, K. K. Gleason, *Adv. Mater.* **2011**, *23*, 3500–3505.
- [11] A. C. Siegel, S. T. Phillips, M. D. Dickey, N. Lu, Z. Suo, G. M. Whitesides, *Adv. Funct. Mater.* **2010**, *20*, 28–35.
- [12] A. W. Martinez, S. T. Phillips, M. J. Butte, G. M. Whitesides, *Angew. Chem.* **2007**, *119*, 1340–1342; *Angew. Chem. Int. Ed.* **2007**, *46*, 1318–1320; A. W. Martinez, S. T. Phillips, G. M. Whitesides, E. Carrilho, *Anal. Chem.* **2010**, *82*, 3–10; Z. H. Nie, C. A. Nijhuis, J. L. Gong, X. Chen, A. Kumachev, A. W. Martinez, M. Narovlyansky, G. M. Whitesides, *Lab Chip* **2010**, *10*, 477–483; N. K. Thom, K. Yeung, M. B. Pillion, S. T. Phillips, *Lab Chip* **2012**, *12*, 1768–1770.
- [13] L. B. Wang, W. Chen, D. H. Xu, B. S. Shim, Y. Y. Zhu, F. X. Sun, L. Q. Liu, C. F. Peng, Z. Y. Jin, C. L. Xu, N. A. Kotov, *Nano Lett.* **2009**, *9*, 4147–4152; P. P. Wang, L. Ge, M. Yan, X. R. Song, S. G. Ge, J. H. Yu, *Biosens. Bioelectron.* **2012**, *32*, 238–243.
- [14] H. Petroski, *The Pencil: A History of Design and Circumstance*, Alfred A. Knopf, New York, **1990**.
- [15] J. L. Bahr, J. M. Tour, *J. Mater. Chem.* **2002**, *12*, 1952–1958; W. Zhang, J. K. Sprafke, M. L. Ma, E. Y. Tsui, S. A. Sydlik, G. C. Rutledge, T. M. Swager, *J. Am. Chem. Soc.* **2009**, *131*, 8446–8454.
- [16] D. A. Britz, A. N. Khlobystov, *Chem. Soc. Rev.* **2006**, *35*, 637–659.
- [17] B. Esser, J. M. Schnorr, T. M. Swager, *Angew. Chem.* **2012**, *124*, 5851–5855; *Angew. Chem. Int. Ed.* **2012**, *51*, 5752–5756; F. Wang, H. W. Gu, T. M. Swager, *J. Am. Chem. Soc.* **2008**, *130*, 5392–5393; F. Wang, Y. Yang, T. M. Swager, *Angew. Chem.* **2008**, *120*, 8522–8524; *Angew. Chem. Int. Ed.* **2008**, *47*, 8394–8396.
- [18] R. Vyas, V. Lakafosis, H. Lee, G. Shaker, L. Yang, G. Orecchini, A. Traille, M. M. Tentzeris, L. Roselli, *IEEE Sens. J.* **2011**, *11*, 3139–3152.
- [19] P. M. Albrecht, J. W. Lyding, *Appl. Phys. Lett.* **2003**, *83*, 5029–5031.
- [20] N. T. Alvarez, C. L. Pint, R. H. Hauge, J. M. Tour, *J. Am. Chem. Soc.* **2009**, *131*, 15041–15048.
- [21] E. Bekyarova, M. Davis, T. Burch, M. E. Itkis, B. Zhao, S. Sunshine, R. C. Haddon, *J. Phys. Chem. B* **2004**, *108*, 19717–19720.
- [22] T. Zhang, S. Mubeen, E. Bekyarova, B. Y. Yoo, R. C. Haddon, N. V. Myung, M. A. Deshusses, *Nanotechnology* **2007**, *18*, 165504–165509.